J. Geogr. Sci. 2017, 27(6): 681-696
DOI: 10.1007/s11442-017-1400-x

Mapping the hotspots and coldspots of ecosystem services in conservation priority setting

LI Yingjie[1], *ZHANG Liwei[1], YAN Junping[1], WANG Pengtao[1], HU Ningke[1], CHENG Wei[2], FU Bojie[2]

1. Department of Geography, Tourism and Environment College of Shaanxi Normal University, Xi'an 710119, China;
2. State Key Laboratory of Urban and Regional Ecology, Research Center for Eco-Environmental Sciences, CAS, Beijing 100085, China

Abstract: Spatial-explicitly mapping of the hotspots and coldspots is a vital link in the priority setting for ecosystem services (ES) conservation. However, little research has identified and tested the compactness and efficiency of their ES hotspots and coldspots, which may weaken the effectiveness of ecological conservation. In this study, based on the RUSLE model and Getis-Ord Gi* statistics, we quantified the variation of annual soil conservation services (SC) and identified the statistically significant hotspots and coldspots in Shaanxi Province of China from 2000 to 2013. The results indicate that, 1) areas with high SC presented a significantly increasing trend as well, while areas with low SC only changed slightly; 2) SC hotspots and coldspots showed an obvious spatial differentiation—the hotspots were mainly spatially aggregated in southern Shaanxi, while the coldspots were mainly distributed in the Guanzhong Basin and Sand-windy Plateau; and 3) the identified hotspots had the highest capacity of providing SC, with 29.6% of the total area providing 59.7% of the total service. In contrast, the coldspots occupied 46.3% of the total area, but only provided 17.2% of the total SC. In addition to conserving single ES, the Getis-Ord Gi* statistics method can also help identify multi-functional priority areas for conserving multiple ES and biodiversity.

Keywords: ecosystem services mapping; soil conservation; spatial clustering; Getis-Ord Gi* statistics; Shaanxi Province

1 Introduction

Ecosystem services (ES) are regarded as an effective communication tool to bridge the knowledge between science, policy making, and practice. Work in this field has gained increasing attention in recent years (Trabucchi *et al*., 2014; Guerra *et al*., 2016). Generally, ES

Received: 2016-03-15 **Accepted:** 2016-07-29
Foundation: National Natural Science Foundation of China, No.41601182; National Social Science Foundation of China, No.14AZD094; National Key Research and Development Plan of China, No.2016YFC0501601; China Postdoctoral Science Foundation, No.2016M592743; Fundamental Research Funds for the Central Universities, No.GK201603078; Key Project of the Ministry of Education of China, No.15JJD790022
Author: Li Yingjie (1990–), specialized in environmental change and ecosystem services. E-mail: lyj@snnu.edu.cn
***Corresponding author:** Zhang Liwei (1985–), Assistant Professor, specialized in landscape ecology and ecosystem services. E-mail: zlw@snnu.edu.cn

are grouped into supporting, provisioning, regulating, and cultural services (MA, 2005; Adhikari and Hartemink, 2016). Soil conservation service (SC) is a critical regulating service supplied by terrestrial ecosystems to prevent soil erosion. It is well known that soil loss is one of the most severe and widespread environmental problems in China, especially in the Loess Plateau (Fu *et al*., 2011). The soil deterioration caused by soil loss brings a series of negative impacts on the fragile ecosystem, threatening the sustainability of the food security and social economy in the region (Fu *et al*., 2005; Fu *et al*., 2011; Guerra *et al*., 2016), which have drawn much attention from the stakeholders who suffered the dilemma (Fu *et al*., 2015). The Chinese central and local governments launched a series of soil and water conservation measures to alleviate this situation, and the Grain-for-Green Program (GfG) is one of the most ambitious and widespread actions to restore vegetation. These kinds of giant projects usually need an enormous investment of manpower and material resources, which may add a great burden to our national economy and consequently restrict the sustainability of the projects. Thus, spatial-explicitly assessing soil conservation is of great importance to convey effective messages to the stakeholders and facilitate targeted decision making. ES mapping, especially the identification of ES hotspots is a primary node bringing ES into the process of ecological conservation assessment.

ES hotspots are defined as regions with high service-diversity, high biophysical or monetary value of services, or high capability of supplying services; the opposite features are defined as coldspots (Li, 2014; Schröterand Remme, 2016). Here, we focus on "hotspot" defined as areas with a high biophysical value of a single service. Identifying hotspots and coldspots can offer a reference for scientifically defining conservation boundary and setting conservation priority area when allocating limited resources in the process of ecosystem management (Reyers *et al*., 2009; Zhang and Fu, 2014). A range of relevant research has been performed by using several priority-setting approaches (Trabucchi *et al*., 2013; Zhang *et al*., 2014), which can be classified into two types. The first one is by defining a certain threshold to determine hotspots and coldspots. For example, Wu *et al*. (2013) defined the top 10% of the grid cell value as the hotspots of that ES. Similarly, Gimona and van der Horst (2007) counted the grid cells values above or below the median value of all grid cells as hotspots. These maneuverable practices can map priority areas and provide references for systematic ecological conservation planning. However, threshold or quantiles-based method usually ignore the landscape connectivity between or within the identified hotspots, which can lead to undesirable and severe landscape fragmentation. Implementing conservation projects in fragmentized patches can be thorny and costly (Mitchell *et al*., 2015). Thus, spatial clustering methods are needed to prevent identifying fragmentary hotspots. Fortunately, another type of method is based on spatial aggregation/clustering analysis, among which, Kernel density estimation (KDE), a frequently used hotspot analysis method can reveal where point or line features are concentrated (Alessa *et al*., 2008). However, the KDE method only takes the location information into the identification but does not put the features' attribute values into the results. Therefore, KDE is only useful for the aggregation of scattered, location-based data (such as the survey data of multiple ES), but is unfit for spatially uniform grid data. In addition, geostatistical analyses, such as Moran's I, Getis-Ord Gi* statistics can also be used to identify hotspots, but in practice, the Getis-Ord Gi* statistics (or Gi* statistics, for short) was proved to be superior to the alternatives

(Braithwaite and Li, 2007). The greatest advantage of the Gi^* statistics is that it takes the value of all neighboring features into consideration and reports hotspots and coldspots with different levels of statistical significance. The output hotspots can present better continuous surface, which is an expression of landscape connectivity. Hotspot analysis using the Gi^* statistics has been widely applied in crime analysis, epidemiology, traffic accidents, economic geography, demographics and similar parameters (Alessa *et al*., 2008; ESRI, 2013; Barro *et al*., 2015); in recent years, it is commonly seen in biodiversity study (O'Farrell *et al*., 2011; Di Minin *et al*., 2013). However, seldom has it been used in the identification of ES conservation priority areas. Although a few "hotspots mapping" can be found in relevant studies by using kernel density estimation or defining a certain threshold (Guerra *et al*., 2016; Li, 2014), these methods are not sufficient from the perspective of statistical significance (Mitchell, 2005), thus are less effective when compared to the Gi^* statistics.

In this study, we use Shaanxi Province as a case study. Based on the RUSLE model and the newly introduced hotspot analysis method (i.e., Gi^* statistics), the objectives of this study are to 1) map and assess the spatio-temporal variations of SC in Shaanxi from 2000 to 2013; 2) identify the hotspots and coldspots of SC and evaluate their capacity of supplying SC; and 3) discuss the driving factors that led to changes in SC. The results and method may contribute to conservation planning as well as support the policy making associated with sustainable land-use planning and ecosystem management.

2 Materials and methodology

2.1 Study area

Shaanxi Province (105°29′–110°15′E, 31°42′–39°35′N) is located in northwest China, with an area of 205.8 thousand km^2 and population of about 37.75 million by the end of 2013 (Figure 1). Characterized by a mainland monsoon climate, the annual precipitation decreases from south to north. The annual precipitation in the Hanjiang River Basin is about 1000 mm, reduces to 800 mm in the Qinling Mountain zone, and is only 400 mm in the Sand-windy Plateau zone. The major soil types in Shaanxi include loessial soil, (yellow) brown soil, cinnamon soil and aeolian sandy soil (Feng, 2013). Terrains of Shaanxi are high in the north and south, and low the middle part of the Guanzhong Basin. The Yellow River Basin and the Yangtze River Basin account for 62.6% and 35.4% of Shaanxi's area, respectively, and approximately 40% of Shaanxi is on the Loess Plateau, where the inappropriate land use and degraded vegetation have made it the most severe soil loss region in China (Jiang *et al*., 2015; Su *et al*., 2012).Under the background of climate change and rapid economic development in recent decades, the ecosystem degradation in Shaanxi has prompted great concern about the conservation of biodiversity and ES (Jia *et al*., 2014). During the past decades, many ameliorative actions, like the Three-North Shelter Forest Program (TNSFP) and the Grain-for-Green Program (GfG), have made great contributions to vegetation restoration and soil loss control in China. However, this kind of program at the physical regionalization scale or watershed scale may invite poor accountability for regional management (Zhang and Song, 2003; Wang *et al*., 2010b). Thus we conducted the research at an administrative regional scale, hoping to facilitate the policy making of ecosystem restoration.

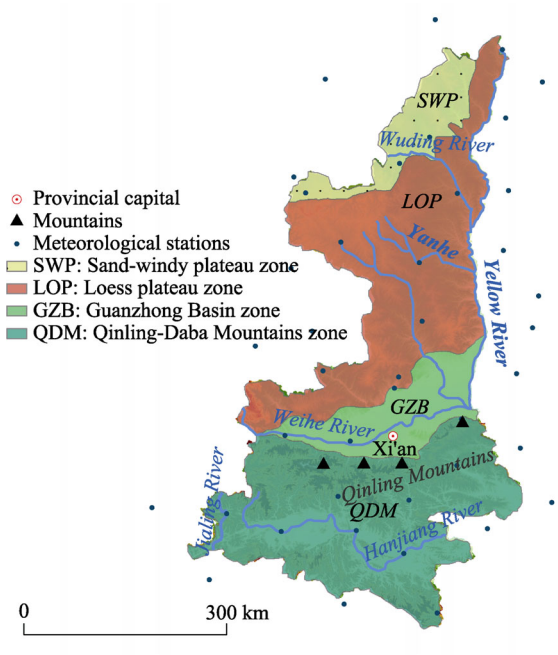

Figure 1 Location of meteorological stations and geographical division in Shaanxi Province, China

2.2 Datasets and methodology

2.2.1 Data sources

The monthly meteorological data (precipitation and temperature) of 45 stations (Figure 1) are retrieved from the website of National Meteorological Information Center. Topographical parameters (i.e. slope, aspect, and elevation) are derived from STRM (Shuttle Radar Topography Mission) DEM data. The soil properties data come from Harmonized World Soil Database (version 1.2). The NDVI (Normalized Difference Vegetation Index) data are acquired from NASA's Earth Observing System. The Land Use and Land Cover (LULC) maps are derived and interpreted from the Landsat Thematic Mapper (TM) data, and we control the accuracy at about 92% by field reconnaissance and Google Earth verification. We resampled all the parameters (listed in Table 1) into 250 m resolution before inputting them into the model simulation.

Table 1 The datasets sources

Data	Type	Resolution	Time period	Sources
Meteorological data	Point	—	2000–2013	http://cdc.cma.gov.cn/
Soil properties	Raster	1 km	2000	http://webarchive.iiasa.ac.at/
DEM	Raster	90 m	2004	http://srtm.csi.cgiar.org/
LULC	Polygon	30 m	2000, 2013	http://www.landcover.org/data/
MODIS NDVI	Raster	250 m	2000–2013	http://ladsweb.nascom.nasa.gov/data/

2.2.2 Method for mapping SC

The staple soil conservation (SC) assessment methods are mainly based on empirical soil erosion models, i.e., the RUSLE (Revised Universal Soil Loss Equation) model (Renard *et al*., 1997; Wischmeier and Smith, 1965; Rao *et al*., 2014), by which soil conservation can be quantified by the difference between potential soil loss and actual soil loss (Li, 2014; Guerra *et al*., 2014; Baró *et al*., 2015).

$$SC = A_p - A_r = R \times K \times L \times S - R \times K \times L \times S \times C \times P \quad (1)$$

where SC is the annual amount of soil conservation ($t \cdot hm^{-2} \cdot yr^{-1}$); A_p presents the annual potential soil erosion without ES supplied (here, vegetation cover), and A_r is annual actual soil loss; other parameters are estimated as follows:

1) R: rainfall erosivity factor ($MJ \cdot mm \cdot hm^{-2} \cdot h^{-1} \cdot yr^{-1}$) is calculated by using the empirical

formula developed by Wischmeier and Smith (1978); the P_i and P are the monthly and annual precipitation (mm) respectively.

$$R = \sum_{i=1}^{12} 1.735 \times 10^{\left(1.5\lg\frac{P_i^2}{P} - 0.8188\right)} \tag{2}$$

2) K: soil erodibility factor ($t \cdot ha \cdot h \cdot ha^{-1} \cdot MJ^{-1} \cdot mm^{-1}$) describes the vulnerability of the soil to raindrop detachment and runoff wash. The calculation is based on the EPIC (Erosion-Productivity Impact Calculator) equation formulated by Sharpley and Williams (1990); the *SAN*, *SIL*, *CLA* and *C* are the percentage (%) of sand, silt, clay and organic matter in soil, and $SNI = 1 - SAN/100$ (Zhang *et al*., 2014)

$$K = \left\{0.2 + 0.3\exp\left[-0.0256SAN\frac{1-SIL}{100}\right]\right\}\left(\frac{SIL}{CLA+SIL}\right)^{0.3} \times \left[1.0 - \frac{0.25C}{C + \exp(3.72 - 2.95C)}\right]\left[1.0 - \frac{0.7SNI}{SNI + \exp(-5.51 + 22.9SNI)}\right] \times 0.1317 \tag{3}$$

3) L: the slope length factor is calculated using formula defined by McCool *et al*. (1987); S stands for slope factor, and m is a dimensionless constant depending on the percent slope (θ).

$$L = \left(\frac{\lambda}{22.13}\right)^m \begin{cases} m = 0.5 & \theta \geqslant 9 \\ m = 0.4 & 9 > \theta \geqslant 3 \\ m = 0.3 & 3 > \theta \geqslant 1 \\ m = 0.2 & 1 > \theta \end{cases} \tag{4}$$

$$S = \begin{cases} 10.8\sin\theta + 0.03 & \theta < 9 \\ 16.8\sin\theta - 0.50 & 9 \leqslant \theta \geqslant 18 \\ 21.91\sin\theta - 0.96 & \theta > 18 \end{cases} \tag{5}$$

4) C: crop and management factor; C is estimated by using Cai *et al*. (2000) model. The f parameter refers to vegetation coverage, which is computed by using NDVI data (Fu *et al*., 2011).

$$C = \begin{cases} 1 & f = 0 \\ 0.6508 - 0.3436\lg f & 0 < f \leqslant 78.3 \\ 0 & f > 78.3 \end{cases} \tag{6}$$

5) P refers to conservation practice factor, which is estimated according to the method applied in Loess Plateau (Lufafa *et al*., 2003; Fu *et al*., 2011). α is the percentile slope gradient and is calculated from DEM.

$$P = 0.2 + 0.03\alpha \tag{7}$$

2.2.3 Gi^* statistics-based hotspots and coldspots analysis

In this paper, the Gi^* statistics was used to identify hotspots and coldspots of soil conservation service (SC). As a tool integrated in ArcGIS 10.2, this approach takes each raster pixel within the context of neighboring features into the calculation and outputs a new feature class with z-score, p-value and confidence level. Features with high z-score and small

p-value indicate statistically significant hotspots, and features with low negative z-score and small p-value demonstrate statistically significant coldspots. The magnitude of the absolute value of the z-score explains the intensity of the clustering (Getis and Ord, 1992; Mitchell, 2005). This approach can help identify hotspots and coldspots with different significant levels, so based on which stakeholders can set corresponding priorities according to the actual requirements. The principle of this method is shown as follows:

$$G_i^* = \frac{\sum_{j=1}^{n} w_{ij}x_j - \overline{X}\sum_{j=1}^{n} w_{ij}}{S\sqrt{\frac{\left[n\sum_{j=1}^{n} w_{ij}^2 - \left(\sum_{j=1}^{n} w_{ij}\right)\right]^2}{n-1}}} \tag{8}$$

where the G_i^* is a z-score of patch *i*. x_j is the attribute value for patch *j*; w_{ij} is the spatial weight between patch *i* and patch *j*, if the distance from a neighbor *j* to the feature *i* is within the distance, $w_{ij} = 1$; otherwise $w_{ij} = 0$; *n* is the total number of grid cells and

$$\overline{X} = \frac{\sum_{j=1}^{n} x_j}{n}, \quad S = \sqrt{\frac{\sum_{j=1}^{n} x_j^2}{n-1} - (\overline{X})^2} \tag{9}$$

Identifying and mapping the hotspots and coldspots can visualize priority areas spatial-explicitly, which is helpful for targeted policy making. Crossman and Bryan (2009) have demonstrated that the conservation benefits could increase by 25% by using hotspots analysis over a random approach.

2.2.4 Other methods

Linear trend analysis has been widely used in analyzing the vegetarian cover change and climate change for a continuous period (Lu *et al*., 2015; Deng *et al*., 2013). In this paper, we adopted linear regression to analyze the changing trend of SC from 2000 to 2013. Also, Kriging spatial interpolation was conducted using the geostatistical analysis module in ArcGIS 10.2 (ESRI, 2013), through which we can adjust the parameters and construct the ideal interpolation model.

3 Results

3.1 Spatio-temporal variations of SC

The spatial patterns of SC show that the amount of SC increased approximately from north to south (Figure 2a). Precisely, divided by Qinling Mountains, the SC in the Guanzhong Basin and Sand-windy Plateau zone was low, while the Qinling-Daba Mountains zone showed high SC.

The total SC in Shaanxi experienced a significant increase at a rate of 0.47 $t \cdot hm^{-2} \cdot a^{-1}$ ($P<0.01$) from 2000 to 2013. It increased from 5.43×10^8 t in 2000 to 14.07×10^8 t in 2013, which generally synchronized with the rainfall. Figures 2b and 2c show the change rate and the significance of changing trend, respectively. The significant increase of SC ($P<0.05$) was

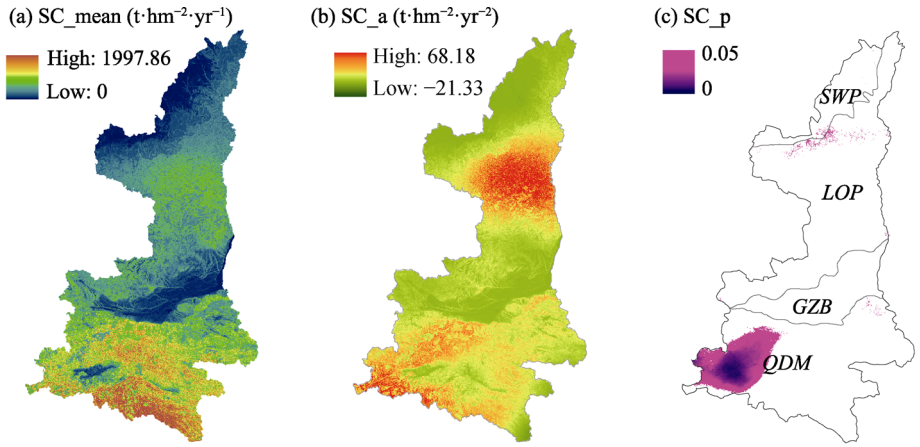

Figure 2 Spatial patterns of SC (a), change rate of SC (b) and the significant (P<0.05) change areas (c) from 2000 to 2013. The change rate at cell level was calculated by using the least square method (LSM).

intensively aggregated in the west of Qinling-Daba Mountains and was sporadically distributed in the north of the Loess Plateau zone. Besides, areas with high SC presented a significant increase while areas with low SC changed slightly.

Since the Grain-for-Green Program (GfG) was launched in 1999, the vegetation restoration has improved a lot. Accordingly, the soil loss control has made great progress in the Loess Plateau, especially in the middle of the Loess Plateau zone. SC's spatial distribution pattern may be closely related to local topography and human activities. Northern Shaanxi is extensively covered by gully and desert, where the structure of loess is relatively loose and the loose loess tends to be eroded by rainfall and the wind. Also, in the arid and semiarid regions, the heterogeneous seasonal precipitation and recurring storms often lead to fragile land cover and low capacity of conserving water and soil. While the Guanzhong Basin is characterized by a low slope and dense population, extensive and intensive human activities have severely altered the land cover; thereby produced a profound influence on the capability of water and soil conversation. However, the Qinling-Daba Mountains zone with slope gradient above 25% in southern Shaanxi provided the most SC. This hilly region accounts for nearly 42.76% of Shaanxi Province, and the population is concentrated in the Hanjiang River Basin. Thus human activities have less impact on the land cover in this region (Zhang *et al*., 2010). Furthermore, abundant rainfall there can ensure the exuberant vegetation, thereby facilitates the soil conservation.

3.2 Hotspots and coldspots of SC

3.2.1 Identifying and mapping hotspots and coldspots

The statistically significant hotspots and coldspots with different confidence levels are shown in Figure 3. Generally, P<0.05 (i.e., 95% confidence level) is defined as statistically significant (Bryan *et al*., 2010). Thus, we focused on hotspots and coldspots with above 95% confidence in this study.

The statistically significant hotspots (hotspots**, for short) of SC accounting for 29.6% of the area of Shaanxi provided 59.7% of the total SC, while the coldspots with above 95% confidence (coldspots**, for short) accounting for 46.3% of the area provided only 17.2% of the

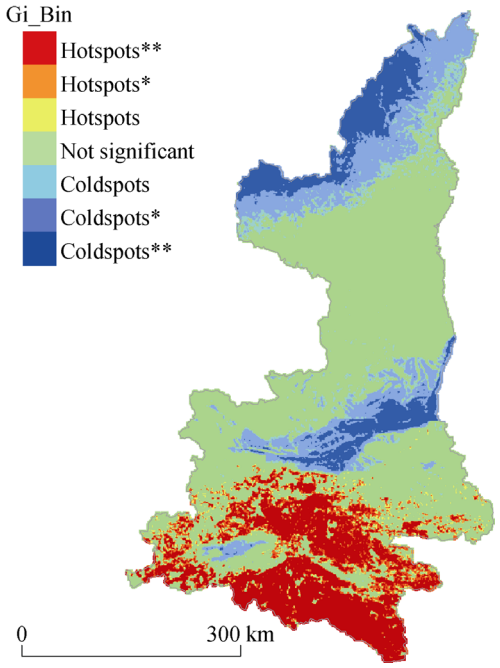

Figure 3 Hotspots and coldspots with different confidence levels (The double star (**) and single star (*) superscript indicate hotspots or coldspots are significant at 99% and 95% level respectively)

total SC (Table 2). The results indicated that the hotspots have the highest capacity of conserving soil. Areas with hotspots** could supply mean amount of 508.08 $t \cdot km^{-2} \cdot a^{-1}$ soil conservation service, which is six times as many as the coldspots**. This high effectiveness of hotspots means implementing conservation project in these areas will be more cost-efficient. This knowledge can facilitate workable policy making and targeted action taking (Guerra *et al*., 2016).

Moreover, the spatial patterns of hotspots and coldspots can guide targeted priority policy making. Hotspots** of SC were mainly scattered in southern Shaanxi (i.e., the QDM zone), while coldspots** were mainly distributed in the Guanzhong Basin and Sand-windy Plateau zone (Figure 3). The results indicated that the supply of soil conservation service was mainly centered in the south of Shaanxi and these hotspots should be well protected in case of being disrupted. However, in the north of Shaanxi, there were few SC hotspots. Encouragingly, the LOP zone, where characterized by the most serious soil loss in the last century, has not seen coldspots in recent 14 years, which also illustrated the positive effects of vegetation restoration projects.

Table 2 Statistics on the hotspots and coldspots of soil conservation service in Shaanxi Province, China

	Annual SC per unit area ($t \cdot hm^{-2} \cdot a^{-1}$)	Area percentage (%)	Annual SC percentage (%)
Coldspots**	80.85	41.40	13.61
Coldspots*	175.99	4.95	3.55
Coldspots	190.68	2.41	1.87
Not Significant	239.34	20.63	20.08
Hotspots	296.79	1.02	1.24
Hotspots*	309.95	1.86	2.34
Hotspots**	508.08	27.73	57.31

Note: The double star (**) and a single star (*) superscript indicate hotspots or coldspots are significant at 99% and 95% level, respectively.

3.2.2 LULC types in hotspots and coldspots

Vegetation cover plays a vital role in ameliorating the degradation of ES (Reyers *et al*., 2009). It can enhance the trapping of rainwater and reduce the kinetic energy of rainfall, thus mitigate the erosion. By regulating the spatial configuration of LULC, we can enhance the conservation of water and soil (Fu *et al*., 2015; Lorencova *et al*., 2013). For the hotspots identified, 78.9% of which were covered by woodland and grassland, while there were only

43.6% of the coldspots covered by vegetation (Figure 4). Also, a total proportion of 45.8% of the coldspots were found in farmland. Thus, the hotspots usually have high vegetation cover.

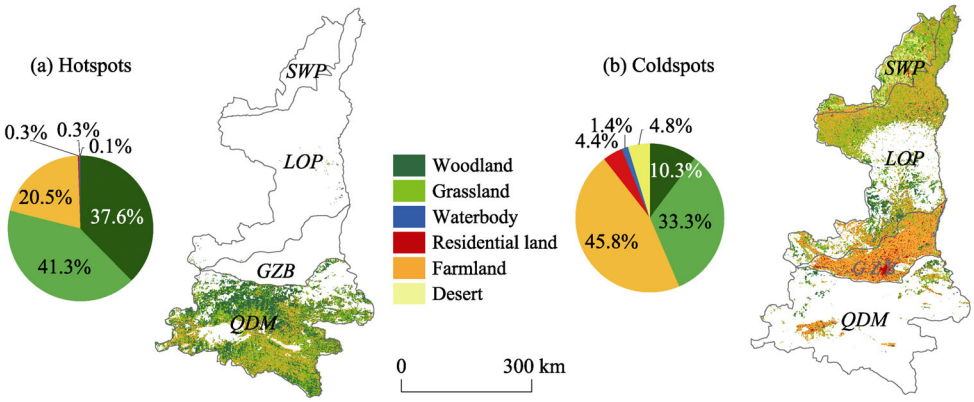

Figure 4 LULC types in hotspots and coldspots. The pie charts indicate the percentage of each LULC from the total area of hotspots or coldspots.

Effective land-use policies can optimize spatial configuration of LULC, thereby influence the provisioning of ES (Fu *et al*., 2015). The SC capacity under different vegetation states reflects the great importance of vegetation for ecosystems, so the hotspots with a high fraction of vegetation cover should be treated as priority reserve where laws and regulations are needed to be reinforced but not too many funds should be invested. As for alleviating coldspots, both policy and funds are required. Regarding the Loess Plateau region, the vegetation restoration and construction like GfG and TNSPF projects should give priority to local or native species to ensure survival rate and long-term ecological effects. For the Guanzhong Basin, where covered by extensive farmland and residential land, more efforts should be placed on irrigation and water conservancy projects, so as to reduce water and soil loss.

4 Discussion

4.1 Driving factors of the SC change

Climate and land use change have been demonstrated to the two main factors that influence the spatio-temporal variation of soil conservation (Su *et al*. 2012, Lorencova *et al*. 2013). In Shaanxi, characterized by fragile underlying surface, intensive human-environment interactions play an increasingly important role in shaping the hydrological processes and sediment export.

4.1.1 LULC change

LULC transition can affect major eco-hydrological processes, including energy exchange, water cycling, soil loss and biogeochemical cycles (Felipe Lucia *et al*., 2014), which directly and indirectly influence the provision of ES (MA, 2005; Fu *et al*., 2015). Due to the joint efforts of GfG and TNSPF, the land cover in northern Shaanxi has changed noticeably (Su and Fu, 2013). Woodland and grassland increased by 1625.33 km^2 and 929.64 km^2 from 2000 to 2013 respectively, and the farmland was reduced by 3780.90 km^2. Meanwhile, the

mean annual SC in each LULC type showed an increasing trend from 2000 to 2013 (Figure 5a). Figure 5b shows the areas and spatial distribution of that other land types transferred to woodland and grassland. The transition was mainly scattered on the middle Loess Plateau zone, which was in accordance with the significant increase of SC in this area. Moreover, we tested the SC supplying capacities of each LULC by applying the Zonal Statistics (ESRI, 2013). The results showed that woodland held the highest capacity of supplying soil conservation service, followed by grassland. In contrast, the capacity of residential land and desert were very low. Therefore, we can conclude that LULC is a key driving force of SC change, which was consistent with Fu *et al*.'s study on the Loess Plateau (Fu *et al*., 2011).

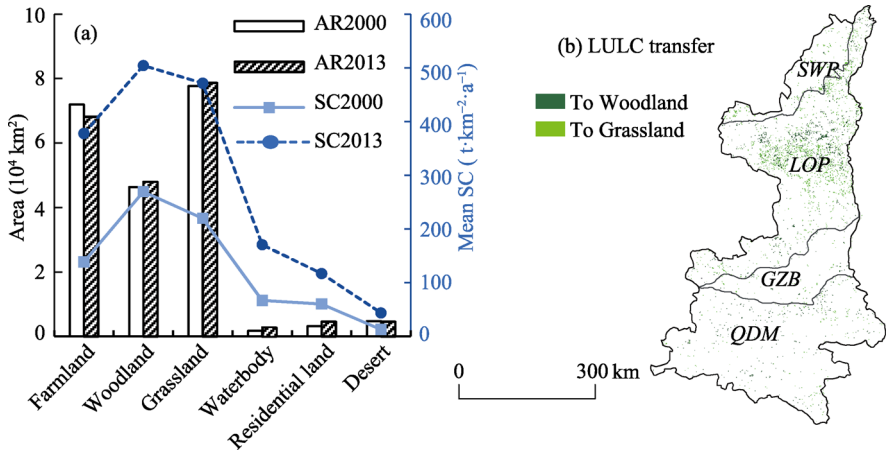

Figure 5 Comparison of LULC change between 2000 and 2013: (a) the area (AR) of LULC change and the mean SC provided by each LULC type; (b) the distribution of other types of LULC transferred to woodland and grassland

4.1.2 Climate change

Though the vegetation restoration projects were widely carried out in China, except the pronounced LULC change in northern Shaanxi, no evident change appeared in the south (Figure 5b). However, the SC in southern Shaanxi did present a significant increasing trend (Figure 2). Therefore, other driving forces, for example, climate change may contribute to the variation of SC. Taking the Yanhe River basin as an example, it was the earliest and fastest region to implement the Grain-for-Green Program (GfG), and the LULC has changed dramatically. Meanwhile, the annual precipitation showed an increasing trend in recent 14 years, which also promoted the growth of vegetation in this arid area (Yapp *et al*., 2010; Fu *et al*., 2011). Thus, the strengthened soil conservation service in this area was the synthetical effects of LULC and climate change. Though the amount of precipitation has been illustrated to be the main driving factor of soil erosion (Fu *et al*., 2011), the precipitation intensity, precipitation frequency and precipitation-concentration-degree and precipitation-concentration-period (Li *et al*., 2016) may also influence the rainfall erosivity (Wei *et al*., 2009; López-Tarazón *et al*., 2010). Thus, the detailed influence mechanism awaits to be further studied.

Particularly, we compared the spatial patterns of SC, precipitation and temperature, and found that the spatial configuration of SC (Figure 2) was similar to precipitation's (Figure 6): both of them showed high values as well as increasing trends in QDM and LOP. Therefore,

apart from the vegetation restoration, climate change might also contribute to the increase of SC in the LOP. Further, the temperature in LOP seemingly tended to decrease in recent 14 years, which may help reduce the vegetational evaporation loss to avoid drought. In this semi-arid and arid area, water is a key factor that constrains the growth of vegetation, and bare or sparsely vegetated ground is prone to be eroded by rainfall. As for southern Shaanxi, especially the west of QDM, both precipitation and temperature showed an evident increasing trend, which was in accordance with the variation of SC. This region is well covered by forest, and little land-cover transfer occurred in the process of vegetation restoration projects. So the significant increase of precipitation may help enhance the SC in the south of Shaanxi.

In conclusion, LULC change under the policy of Grain-for-Green in northern Shaanxi was an incontrovertible driving force of SC increase. Meanwhile, the increasing precipitation in recent years also contributed to this improvement.

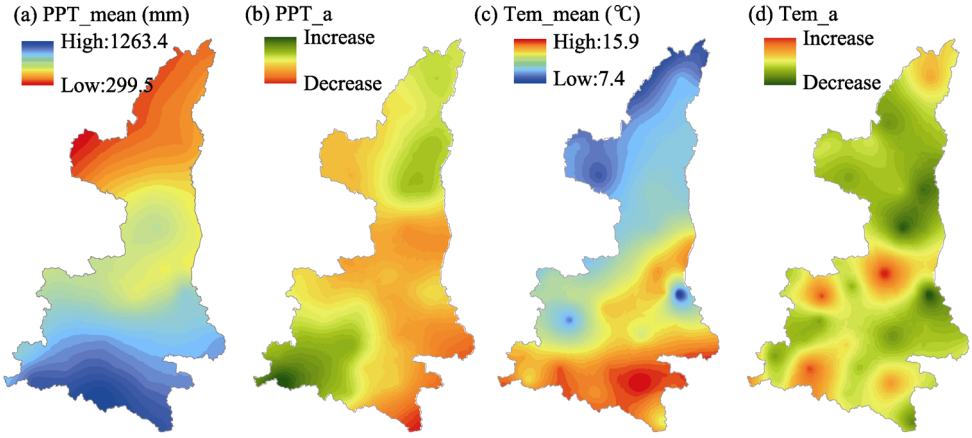

Figure 6 Spatial patterns of mean annual precipitation (PPT) (a), temperature (Tem) (c) and their change rates (b and d) from 2000 to 2013. The change rate at grid cell level was calculated by using the least square method (LSM).

4.2 Why using the Getis-Ord Gi* statistics for hotspots analysis?

Though several spatial clustering analyses (such as KDE, Local Moran's I) can help identify hotspots, the alternatives are all insufficient compared with the Gi* statistics. Kernel density estimation (KDE) is efficient for the scattered, location-based data (such as random investigation data of multiple ES as seen in Figure 7a), but for spatially uniform grid data, it loses efficiency (see Figure 7b). Besides, KDE can only show the location of the clusters, but cannot tell whether the clusters are significant or not. Local Moran's I is more suitable for finding statistically significant clusters of high (or low) values and the outlier (ESRI, 2013), such as figuring out the sharp boundaries between rich and poor in a certain region, or the location of unexpectedly high rates of disease across the study area (ESRI, 2013). This statistic method underlines the level of events of each individual feature of a neighborhood, instead of the combined level of events for the neighborhood as a whole (Braithwaite and Li, 2007), so it is less sensitive to spatial weights among features. Furthermore, unlike epidemic or crime in social science (Eck *et al*., 2005; Braithwaite and Li, 2007; Ahmad *et al*., 2015),

research objects in natural science (for example, SC in this text) are generally homogeneous and have continuous surface and good connectivity. Thus, we do not focus on outlier but on good landscape connectivity for cost-efficient management.

The Gi* statistics is one of the spatial clustering methods, which works by calculating the local sum for a feature and its neighbors and then comparing the preliminary result proportionally to the sum of all features. When the calculated local sum is diametrically different from the expected one, and that difference beyond a random chance, then a statistically significant z-score (i.e., Gi) outputs (ESRI, 2013). Therefore, the Gi* statistics is a more robust method for identifying hotspots and coldspots.

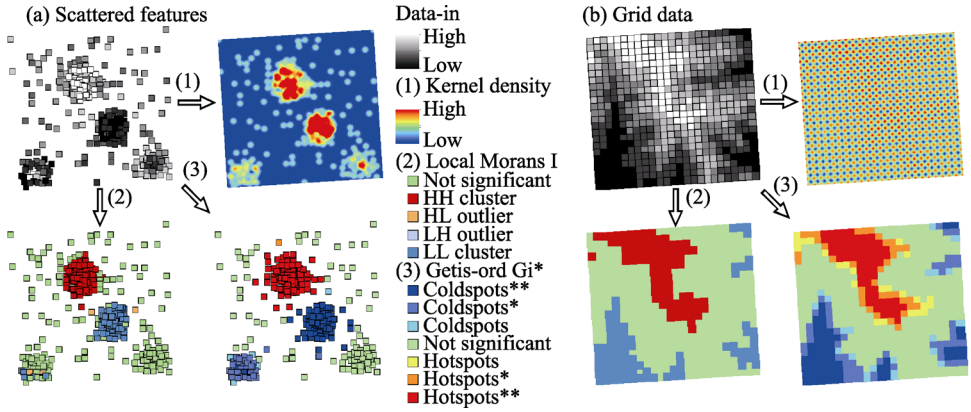

Figure 7 Comparison of three hotspot analysis methods: KDE (1), Local Moran's I (2), Getis-Ord Gi* statistics (3)
Note: When input features are spatially scattered (see Figure 7a), the KDE can only identify spatial cluster, but it mixes the cluster of high values (i.e., hotspots) and the cluster of low values (coldspots); that is, the KDE can neither tell what the cluster is nor whether it is significant. Fortunately, the Local Moran's I and Getis-Ord Gi* statistics can both make it. The difference is that the Local Moran's I is more efficient at identifying the outliers (see Figure 7a-(2) above), while the Gi* statistics is even better at identifying statistically significant hotspots and coldspots with different confidence levels (see Figure 7a-(3)). When input features are spatially uniform grid data (see Figure 7b), the KDE becomes inefficient, while the Local Moran's I and Gi* statistics work well in this case, and the Gi* statistics especially holds its unique superiority.

4.3 Implications of the hotspots and coldspots mapping for conserving ES

While ES mapping can provide guidance for conservation policy making, we propose that hotspots and coldspots analysis should be integrated into the priority area setting for systematic conservation. Prioritization sites with ES hotspots are considered to be comprehensive, compact and cost-effective (Schröter and Remme, 2016). In reality, the conservation budgets are usually not sufficient to conserve all sites. To achieve cost-effectiveness, the hotspots must be compact and with low edge-to-area ratio. Hotspots identified based on quantiles and threshold method are quite fragmented and isolated (Schröter and Remme, 2016), which are in poor quality for reserve networks. But the Gi* statistics-based hotspot analysis method, one of the spatial-clustering quantitative method, is especially efficient for assessing and identifying ES hotspots and coldspots with good spatial connectivity. Thereby, this method is more beneficial for practical and cost-effective ES conservation management (Guerra *et al*., 2014; Moilanen *et al*., 2014).

ES hotspots maps can be used as visual and vivid tools to initiate communications with stakeholders about management planning (Maes *et al*., 2013). Clarifying the hotspots and coldspots sites helps set priorities for maintaining essential ES when financial resources are limited (de Groot *et al*., 2010; Newburn *et al*., 2005; Crossman and Bryan, 2009). ES hotspots should get the priorities of being reserved and avoid being damaged; as for ES coldspots, targeted measures should be taken to ameliorate the severe status quo by analyzing and sorting out local drivers of ES conflicts and degeneration (Jiang *et al*., 2013). In this text, the SC hotspots mainly occurred in areas with high vegetation cover, while SC coldspots mostly appeared in areas covered by farmland (Figure 4). With this knowledge, we suggest that the Grain for Green Program should continue to be implemented in the coldspots areas.

For different purposes of ES conservation, there are different definitions for ES hotspot. As for Shaanxi Provence, soil loss is one of the most serious environmental problems in this area, so we focus on a single service and identify the SC hotspots and coldspots to set priorities for conservation. But our ecosystems are often complex, and one landscape usually holds several functions and services. Thus, multiple ES should be considered at a time to conserve multi-functional hotspots. The Gi^* statistics-based hotspots analysis is also efficient for this case (Schröter and Remme, 2016).

5 Conclusions

To achieve efficient ecosystem conservation, we need to find out the optimal scheme for resource allocation. ES hotspots and coldspots mapping provides a pathway for conservation priority setting. By integrating several spatial datasets and models, this case study examined the spatio-temporal variation of the soil conservation service for Shaanxi Province, and further mapped the ES hotspots and coldspots based on Getis-Ord Gi^* statistics method.

The results showed that the annual SC in Shaanxi experienced an evident increasing tendency from 2000 to 2013 as a whole, but the changes in SC and its drivers were spatially heterogeneous. We found that the increase of SC in northern Shaanxi was mainly due to LULC change, while in the south, the increase was mainly affected by precipitation.

Furthermore, our study pointed out that Gi^* statistics has the potential to guide conservation priority setting, since this method can help identify ES hotspots and coldspots with high landscape connectivity and compactness. Hotspots identified using the method have a much higher capacity of supplying ES compared with the non-hotspots. This means protecting less area (i.e., hotspots) can benefit more service. Thus, this study offered a cost-efficient and spatially-explicit framework for ES conservation priority setting. Stakeholders can also integrate this method into their framework for identifying and conserving multi-functional hotspots of ES or biodiversity to support targeted ecosystem policy making.

Acknowledgments

We are grateful to the anonymous reviewers for their constructive advice about the paper, and we also thank Chen Guoyong from the Hunan University, who provided important aid in calculating the annual soil conservation of Shaanxi by MATLAB programming.

References

Adhikari K, Hartemink A E, 2016. Linking soils to ecosystem services: A global review. *Geoderma*, 262: 101–111.

Ahmad S, Aziz N, Butt A *et al*., 2015. Spatio-temporal surveillance of water based infectious disease (malaria) in Rawalpindi, Pakistan using geostatistical modeling techniques. *Environmental Monitoring and Assessment*, 187(9): 1–15.

Alessa L, Kliskey A, Brown G, 2008. Social-ecological hotspots mapping: A spatial approach for identifying coupled social-ecological space. *Landscape and Urban Planning*, 85(1): 27–39.

Baró F, Haase D, Gómez-Baggethun E *et al*., 2015. Mismatches between ecosystem services supply and demand in urban areas: A quantitative assessment in five European cities. *Ecological Indicators*, 55: 146–158.

Barro A S, Kracalik I T, Malania L *et al*., 2015. Identifying hotspots of human anthrax transmission using three local clustering techniques. *Applied Geography*, 60: 29–36.

Braithwaite A, Li Q, 2007. Transnational terrorism hot spots: Identification and impact evaluation. *Conflict Management and Peace Science*, 24(4): 281–296.

Bryan B A, Raymond C M, Crossman N D *et al*., 2010. Targeting the management of ecosystem services based on social values: Where, what, and how? *Landscape and Urban Planning*, 97(2): 111–122.

Burkhard B, Kroll F, Müller F *et al*., 2009. Landscapes' capacities to provide ecosystem services: A concept for land-cover based assessments. *Landscape Online*, 15(1): 22.

Cai Chongfa, Ding Sshuwen, Shi Zhihua *et al*., 2000. Study of applying USLE and geographical information system IDRISI to predict soil erosion in small watershed. *Journal of Soil and Water Conservation*, 14(2): 19–24. (in Chinese)

Crossman N D, Bryan B A, 2009. Identifying cost-effective hotspots for restoring natural capital and enhancing landscape multifunctionality. *Ecological Economics*, 68(3): 654–668.

de Groot R S, Alkemade R, Braat L *et al*., 2010. Challenges in integrating the concept of ecosystem services and values in landscape planning, management and decision making. *Ecological Complexity*, 7(3): 260–272.

Deng Shaofu, Yang Taibao, Zeng Biao *et al*., 2013. Vegetation cover variation in the Qilian Mountains and its response to climate change in 2000–2011. *Journal of Mountain Science*, 10(6): 1050–1062.

Di Minin E, Hunter L T, Balme G A *et al*., 2013. Creating larger and better connected protected areas enhances the persistence of big game species in the maputaland-pondoland-albany biodiversity hotspot. *PloS One*, 8(8): e71788.

Eck J, Chainey S, Cameron J *et al*., 2005. Mapping Crime: Understanding Hot Spots. USA: *National Institute of Justice*. Available online at http://www.ojp.usdoj.gov/nij.

ESRI, 2013. ArcGISDesktop: Release 10.2. Redmond, CA: Esri Inc.

Felipe Lucia M, Comín F A, Bennett E M, 2014. Interactions among ecosystem services across land uses in a floodplain agroecosystem. *Ecology and Society*, 19(1): 20.

Feng Lei, 2013. Study on the soil and water conservation function regionalization of Shaanxi Province [D]. Beijing: Beijing Forestry University. (in Chinese)

Fu B, Liu Y, Lü Y *et al*., 2011. Assessing the soil erosion control service of ecosystems change in the Loess Plateau of China. *Ecological Complexity*, 8(4): 284–293.

Fu B, Zhang L Xu Z *et al*., 2015. Ecosystem services in changing land use. *Journal of Soils and Sediments*, 15(4): 833–843.

Fu B, Zhao W, Chen L *et al*., 2005. Assessment of soil erosion at large watershed scale using RUSLE and GIS: A case study in the Loess Plateau of China. *Land Degradation & Development*, 16(1): 73–85.

Getis A, Ord J K, 1992. The analysis of spatial association by use of distance statistics. *Geographical Analysis*, 24(3): 189–206.

Gimona A, van der Horst D, 2007. Mapping hotspots of multiple landscape functions: A case study on farmland afforestation in Scotland. *Landscape Ecology,* 22(8): 1255–1264.

Guerra C A, Maes J, Geijzendorffer I *et al*., 2016. An assessment of soil erosion prevention by vegetation in Mediterranean Europe: Current trends of ecosystem service provision. *Ecological Indicators*, 60: 213–222.

Guerra C A, Pinto-Correia T, Metzger M J, 2014. Mapping soil erosion prevention using an ecosystem service modeling framework for integrated land management and policy. *Ecosystems*, 17(5): 878–889.

Jacobs S, Burkhard B, Van Daele T *et al*., 2015. 'The Matrix Reloaded': A review of expert knowledge use for mapping ecosystem services. *Ecological Modelling*, 295: 21–30.

Jia X, Fu B, Feng X *et al*., 2014. The tradeoff and synergy between ecosystem services in the Grain-for-Green areas in Northern Shaanxi, China. *Ecological Indicators*, 43: 103–113.

Jiang M, Bullock J M, Hooftman D A P *et al*., 2013. Mapping ecosystem service and biodiversity changes over 70 years in a rural English county. *Journal of Applied Ecology*, 50(4): 841–850.

Jiang R, Xie J, He H *et al*., 2015. Use of four drought indices for evaluating drought characteristics under climate change in Shaanxi, China: 1951–2012. *Natural Hazards*, 75(3): 2885–2903.

López-Tarazón J, Batalla R, Vericat D *et al*., 2010. Rainfall, runoff and sediment transport relations in a mesoscale mountainous catchment: The River Isábena (Ebro basin). *Catena*, 82(1): 23–34.

Li Shuangcheng, 2014. The Geography of Ecosystem Services. The Geography of Ecosystem Services. Beijing: Science Press, 75–79. (in Chinese)

Li Yingjie, Yan Junping, Liu Yonglin, 2016. Research on the relationship between dryness/wetness and precipitation heterogeneity in north and south of the Qinling Mountains. *Arid Zone Research*, 33(3): 619–627. (in Chinese)

Lorencova E, Frelichova J, Nelson E *et al*., 2013. Past and future impacts of land use and climate change on agricultural ecosystem services in the Czech Republic. *Land Use Policy*, 33: 183–194.

Lü Y, Zhang L, Feng X *et al*., 2015. Recent ecological transitions in China: Greening, browning, and influential factors. *Scientific Reports*, 5: 8732.

Lufafa A, Tenywa M, Isabirye M *et al*., 2003. Prediction of soil erosion in a Lake Victoria basin catchment using a GIS-based Universal Soil Loss model. *Agricultural Systems*, 76(3): 883–894.

MA [Millenium Ecosystem Assessment], 2005. Ecosystems and Human Well-Being: Current State and Trends. Washington, DC Island Press.

Maes J, Teller A, Erhard M *et al*., 2013. Mapping and assessment of ecosystems and their services: An analytical framework for ecosystem assessmentsunder action 5 of the EU biodiversity strategy to 2020. Luxembourg: Publications Office of the European Union.

McCool D K, Brown L C, Foster G R *et al*., 1987. Revised slope steepness factor for the Universal Soil Loss Equation. *Transactions of the ASAE*, 30(5): 1387–1396.

Mitchell A, 2005. The ESRI Guide to GIS Analysis, Volume 2: Spatial Measurements and Statistics. Redlands. CA: Esri Press.

Mitchell M G, Suarez-Castro A F, Martinez-Harms M *et al*., 2015. Reframing landscape fragmentation's effects on ecosystem services. *Trends in Ecology & Evolution*, 30(4): 190–198.

Moilanen A *et al*., 2014. Zonation spatial conservation planning framework and software v.4.0, User Manual. Biodiversity Conservation Informatics Group, Department of Biosciences, University of Helsinki, Finland. http://cbig.it.helsinki.fi/files/zonation/ (Date of access: 01/03/2016).

Newburn D, Reed S, Berck P *et al*., 2005. Economics and landuse change in prioritizing private land conservation. *Conservation Biology*, 19(5): 1411–1420.

O'Farrell P J, De Lange W J, Le Maitre D C *et al*., 2011. The possibilities and pitfalls presented by a pragmatic approach to ecosystem service valuation in an arid biodiversity hotspot. *Journal of Arid Environments*, 75(6): 612–623.

Rao E, Ouyang Z, Yu X *et al*., 2014. Spatial patterns and impacts of soil conservation service in China. *Geomorphology*, 207: 64–70.

Renard K G, Foster G, Weesies G *et al*., 1997. Predicting soil erosion by water: A guide to conservation planning with the Revised Universal Soil Loss Equation (RUSLE). United States Department of Agriculture Washington, DC.

Reyers B, O'Farrell P J, Cowling R M *et al*., 2009. Ecosystem services, land-cover change, and stakeholders: Finding a sustainable foothold for a semiarid biodiversity hotspot. *Ecology and Society*, 14(1): 38. URL: http://www.ecologyandsociety.org/vol14/iss1/art38/.

Schröter M, Remme R P, 2016. Spatial prioritisation for conserving ecosystem services: Comparing hotspots with heuristic optimisation. *Landscape Ecology*, 31(2): 431–450.

Sharpley A N, Williams J R, 1990. EPIC-erosion/productivity impact calculator: 1. Model documentation. *Technical Bulletin-United States Department of Agriculture*, 1768: 235.

Su C, Fu B, 2013. Evolution of ecosystem services in the Chinese Loess Plateau under climatic and land use changes. *Global and Planetary Change*, 101: 119–128.

Su C, Fu B J, He C *et al*., 2012. Variation of ecosystem services and human activities: A case study in the Yanhe Watershed of China. *Acta Oecologica*, 44: 46–57.

Trabucchi M, Comin F A, O'Farrell P J, 2013. Hierarchical priority setting for restoration in a watershed in NE Spain, based on assessments of soil erosion and ecosystem services. *Regional Environmental Change,* 13(4): 911–926.

Trabucchi M, O'Farrell P J, Notivol E *et al*., 2014. Mapping ecological processes and ecosystem services for prioritizing restoration efforts in a semi-arid Mediterranean river basin. *Environmental Management*, 53(6): 1132–1145.

Wang Xiaofeng, Chang Junjie, Yu Zhengjun *et al*., 2010a. Research on water disrict of soil erosion based on RUSLE: Take the South-North Diversion Middle Route Project in Shaanxi for example. *Journal of Northwest University* (*Natural Science Edition*), 40(3): 545–549. (in Chinese)

Wang X M, Zhang C X, Hasi E *et al*., 2010b. Has the Three Norths Forest Shelterbelt Program solved the desertification and dust storm problems in arid and semiarid China? *Journal of Arid Environments*, 74(1): 13–22.

Wei W, Chen L, Fu B, 2009. Effects of rainfall change on water erosion processes in terrestrial ecosystems: A review. *Progress in Physical Geography*, 33(3): 307–318.

Wischmeier W, Smith D, 1965. Rainfall-erosion losses from cropland east of the Rocky Mountains, guide for selection of practices for soil and water conservation. *Agriculture Handbook*, 282–295.

Wu J, Feng Z, Gao Y *et al*., 2013. Hotspot and relationship identification in multiple landscape services: A case study on an area with intensive human activities. *Ecological Indicators*, 29: 529–537.

Yapp G, Walker J, Thackway R, 2010. Linking vegetation type and condition to ecosystem goods and services. *Ecological Complexity*, 7(3): 292–301.

Zhang Liwei, Fu Bojie, 2014. The progress in ecosystem services mapping: A review. *Acta Ecologica Sinica*, 34(2): 316–325. (in Chinese)

Zhang L, Fu B, Lü Y *et al*., 2015. Balancing multiple ecosystem services in conservation priority setting. *Landscape Ecology*, 30(3): 535–546.

Zhang Lixiao, Song Yuqin, 2003. Efficiency of the Three-North Forest Shelterbelt Program. *Acta Scicentiarum Naturalum Universitis Pekinesis*, 39(4): 594–600. (in Chinese)